Cell Cycle 11:4, 785-796; February 15, 2012; © 2012 Landes Bioscience

MiR-205 determines the radioresistance of human nasopharyngeal carcinoma by directly targeting PTEN

Changju Qu,[1,2] Zhihui Liang,[3] JiaLing Huang,[4] Ruiying Zhao,[2] Chunhui Su,[2] Sumei Wang,[1] Xudan Wang,[1] Rong Zhang,[3] Mong-Hong Lee[2,*] and Huiling Yang[1,*]

[1]Department of Pathophysiology; Zhongshan School of Medicine; [3]State Key Laboratory of Oncology in South China; Sun Yat-sen University; Guangzhou, China; [2]Department of Molecular and Cellular Oncology; University of Texas MD Anderson Cancer Center; Houston, TX; [4]Division of Infectious Diseases; University of Pennsylvania; Philadelphia, PA USA

Key words: nasopharyngeal carcinoma, PTEN, miRNA, miR-205, radioresistance

Radiotherapy is the primary treatment for nasopharyngeal carcinoma (NPC), but radioresistance severely reduces NPC radiocurability. Here, we have established a radio-resistant NPC cell line, CNE-2R, and investigate the role of miRNAs in radioresistance. The miRNAs microarray assay reveals that miRNAs are differentially expressed between CNE-2R and its parental cell line CNE-2. We find that miR-205 is elevated in CNE-2R. A target prediction algorithm suggests that miR-205 regulates expression of PTEN, a tumor-suppressor. Introducing miR-205 into CNE-2 cells suppresses PTEN protein expression, followed by activation of AKT, increased number of foci formation and reduction of cell apoptosis post-irradiation. On the other hand, knocking down miR-205 in CNE-2R cells compromises the inhibition of PTEN and increases cell apoptosis. Significantly, immunohistochemistry studies demonstrate that PTEN is downregulated at late stages of NPC, and that miR-205 is significantly elevated followed the radiotherapy. Our data conclude that miR-205 contributes to radioresistance of NPC by directly targeting PTEN. Both miR-205 and PTEN are potential predictive biomarkers for radiosensitivity of NPC and may serve as targets for achieve successful radiotherapy in NPC.

Introduction

Radiotherapy is the primary treatment for patients with NPC.[1] NPC tends to be more sensitive to radiation than some other cancers, but success of the therapy depends heavily on tumor stage.[2,3] It is well-documented that the 5-y survival rate of stage I and II NPC ranges from 72% to 90%.[2,3] In contrast, the 5-y survival rates drop to 55% in stage III and 30% in stage IV of the disease, as incidence of local recurrence is relatively high in advanced NPC.[2,3] In fact, radioresistance leading to local recurrence remains a major obstacle to successful treatment in NPC.[4,5] However, the molecular mechanisms responsible for the radioresistance of NPC are not clear yet.

MiRNAs are a family of highly conserved, small noncoding RNAs that post-transcriptionally repress gene expression via degradation or translational inhibition of their target mRNAs. There is mounting evidence suggesting that miRNAs are involved in nearly all physiological and pathological processes[6] and many types of cancer such as breast cancer.[7] Some miRNAs play key roles in tumorigenesis, progression, invasion or metastasis of NPC, such as miR-141, miR-29c, miR-26a, miR-218, miR-200a, miR-10b and others.[8-11] Some miRNAs are involved in radioresistance of other tumors, such as let-7, miR-181a and others,[12,13] but the function of miRNAs on NPC radioresistance is largely unknown.

Here, we report that IR induces expression of miR-205 in NPC, which targets tumor suppressor PTEN and consequently activates the PI3K/Akt pathway, leading to increase of NPC radioresistance. Our findings suggest that miR-205 and PTEN are potential biomarkers to estimate NPC response to radiotherapy and help to identify subgroups of patients that may benefit from personalized therapeutic strategies.

Results

Establishing a radio-resistant NPC cell line. To generate a radio-resistant cell line, we exposed CNE-2 cells in exponential growth phase to a range of doses of IR (2, 4 and 6 Gy), each delivered three times at a dose rate of 101.38 cGy/min. An interval of 3 to 8 weeks between each IR allowed the surviving cells to regenerate. The whole process of IR and culture lasted for about 1 y, and we refer to the surviving cell line as CNE-2R. To verify phenotypes, we irradiated CNE-2R cells and examined them by survival foci formation assay. CNE-2R and CNE-2 cells were irradiated with 0, 2, 4 and 6 Gy and examined by survival foci formation assay. In comparison to CNE-2, CNE-2R showed no change of foci formation ability when IR was absent but gained more foci formation and higher survival fractions when exposed to IR (**Fig. 1A–C**). The effect of IR on cell growth was examined

*Correspondence to: Mong-Hong Lee and Huiling Yang; Email: mhlee@mdanderson.org and hlyangsums@hotmail.com
Submitted: 10/06/11; Revised: 12/27/11; Accepted: 12/30/11
http://dx.doi.org/10.4161/cc.11.4.19228

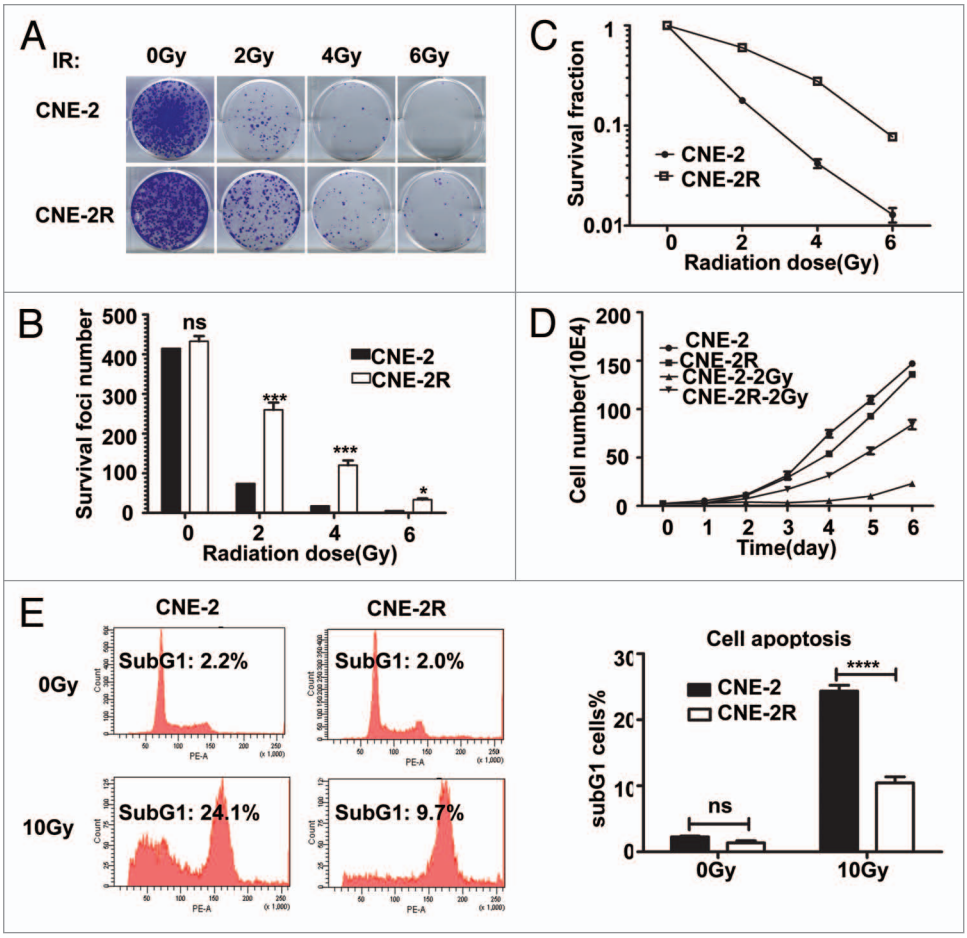

Figure 1. CNE-2R is radio-resistant. (A) CNE-2R is more IR resistant than CNE-2. Indicated cell lines were treated with indicated amounts of irraditiation and forci-formation was indicated. (B) CNE-2R has reduced numbers of forci formation. Indicated cells were plated in triplicate and exposed to a range of IR doses (0–6 Gy). The numbers of foci-formation were presented as bar graphs. (C) CNE-2R has reduced survival fraction. Survival fractions were calculated by dividing the number of colonies formed after IR by the corresponding number of colonies formed without IR from experiments in (B). (D) Growth of CNE-2R is not affected by IR. CNE-2 and CNE-2R plated in 24-well culture plates were exposed to IR with 2 Gy and cell growth was monitored by counting cell numbers. (E) CNE-2R is resistant to IR-induced cell death. The cells were treated with or without 10 Gy IR for analysis of apoptosis of CNE-2 and CNE-2R cells after IR. At 48 h post-irradiation, the cells were stained with PI and the percentage of sub-G_1 cells was measured by flow cytometry in three independent experiments. ns, no significance; *$p < 0.05$; ***$p < 0.001$, ****$p < 0.0001$. Data were presented as mean ± SD.

by subjecting CNE-2R and parent CNE-2 cells to 2 Gy IR. As shown in **Figure 1D**, the CNE-2R cell line had more cell numbers than CNE-2 after IR with 2 Gy. Indeed, the CNE-2 line required 72 h to achieve a 2-fold increase in cell number, while CNE-2R required only 24 h.

We used flow cytometry to determine whether cell apoptosis accumulated for the radioresistance of CNE-2R cells after IR exposure by quantifying the number of cells in sub-G_1 phase as an indicator of apoptosis. Without IR, there was no difference between CNE-2R and CNE-2 in their fractions of sub-G_1 phase cells. In sharp contrast, at 48 h after IR with 10 Gy, the fraction of sub-G_1 phase cells was much lower in CNE-2R cells (**Fig. 1E**). These results indicate that CNE-2R is much more radio-resistant than its parent CNE-2 cells. Moreover, CNE-2R has maintained its radioresistance over 50 passages in the absence of IR (data not shown). We conclude that we have established CNE-2R as a stable radioresistant cell line.

MiR-205 is elevated in radioresistant NPC cells. We used the miRNA microarray approach to determine miRNA expression profiles for both CNE-2R and CNE-2 cell lines (**Fig. 2A**). The results revealed that they had distinct miRNA expression patterns. Among all the 719 individual miRNAs represented on the μParaflo™ miRNA microarrays, we found 37 miRNAs that were dramatically upregulated and 29 miRNAs significantly downregulated in CNE-2R cells when compared with CNE-2 cells (**Fig. 2B**). The change in amplitude ranged from 0.36- to 4.87-fold. We then confirmed the data using qRT-PCR. The miRNAs with one detective value > 1,300 and an absolute value of two detected value ratios (log2 transformed, balanced) > 1 were chosen for assessing miRNA expression by qRT-PCR. The results validated eight miRNAs whose expression levels (**Fig. 2C**) were significantly different between CNE-2R and CNE-2 cells ($p < 0.05$). Specifically, miR-224, let-7g and miR-205 were upregulated, while miR-103, miR-19b, miR-93, miR-24 and miR-18a were downregulated in CNE-2R (**Fig. 2C**). Among the eight miRs, miR-205 was the most abundantly expressed in radio-resistant CNE-2R cells (**Fig. 2C**).

To examine the effect of IR on miR-205 expression in NPC cells, we exposed both CNE-2R and CNE-2 cells to IR (10 Gy) for various periods. As detected by qRT-PCR, miR-205 was significantly increased as early as 1 h after IR in CNE-2R but not in CNE2, indicating that miR-205 is an early responsive gene induced in CNE-2R. Moreover, miR-205 expression level in CNE-2R that responded to IR was much higher in CNE-2R than that in CNE-2 at all time points after IR (**Fig. 2D**). Obviously, induction of miR-205 expression by IR is much faster and stronger in CNE-2R compared with that in CNE-2 cells. In summary, IR induced miR-205 expression, and this induction further amplified the existing difference in miR-205 levels between CNE-2R and CNE-2 cells.

Expression of miR-205 in radiosensitive cells leads to IR resistance. In order to examine the effect of miR-205 on

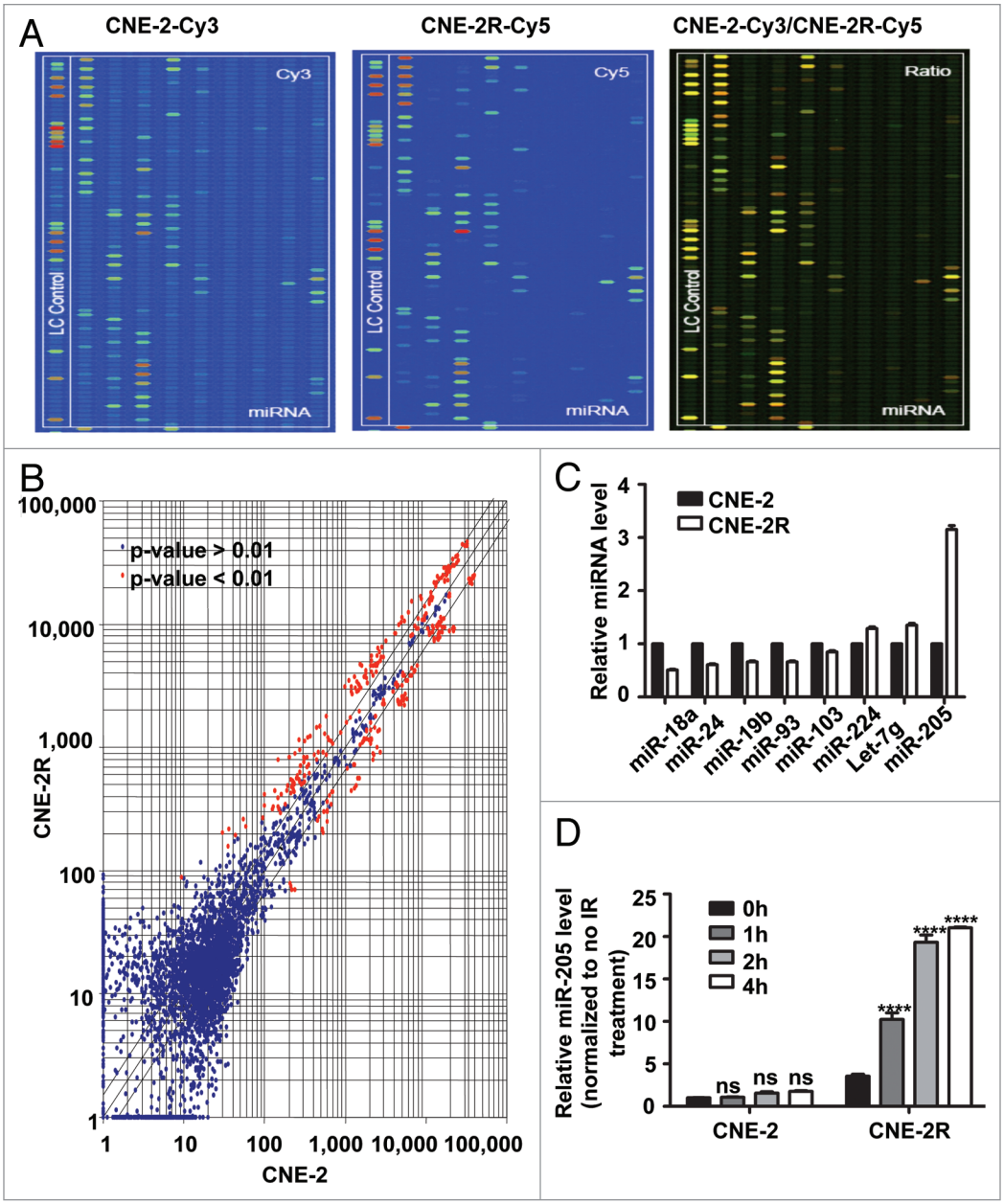

Figure 2. miR-205 is elevated in radio-resistant NPC cells. (A) miR expressing signals from CNE-2 or CNE-2R. miRNAs from CNE-2 or CNE-2R were labeled with Cy3 or Cy5 respectively. (B) Scatter plot of miR expression profiles in radiosensitive CNE-2 (x-axis) and radio-resistant CNE-2R cells (y-axis). The miRs differentially expressed with statistical significance were marked in red. (C) Differential miR expression between CNE-2 and CNE-2R. Relative expression levels of several representative miRs with differential expression levels were presented. (D) Relative miR-205 expression level is different between CNE-2 and CNE-2R after IR. Quantification by qRT-PCR of miR-205 expression level in CNE-2R and CNE-2 cells before and after IR. U6 was used for normalization. Data were presented as mean ± SEM (n = 3). ns, no significance; *p < 0.05; **p < 0.01; ***p < 0.001.

radioresistance in NPC, we generated a CNE-2 cell line stably overexpressing miR-205 (CNE-2/miR-205) (**Fig. 3**). Also, control cells (CNE-2/vector, C) were generated by transducing the CNE-2 with corresponding empty vectors. qRT-PCR confirmed that CNE-2/miR-205 cells had 110-fold increase in miR-205 expression (**Fig. 3A**). With these cell lines in hand, we first measured the effect of miR-205 on the survival foci formation ability and apoptosis when exposed to IR. CNE-2/miR-205 cells had more foci numbers when compared with CNE-2/vector cells (**Fig. 3B and C**). As expected, CNE-2/miR-205 cells have a better survival rate and lower percentage of sub-G_1 when compared with CNE-2/vector cells (**Fig. 3D and E**). Together, these data indicated that overexpression of miR-205 confers radioresistance onto radiosensitive NPC cells.

Suppression of miR-205 in CNE-2R cells leads to radiosensitivity to IR-regulated cell death. Because CNE2-R cells have elevation of miR-205, we then investigated the contribution of miR-205 in radioresistance by knocking down the

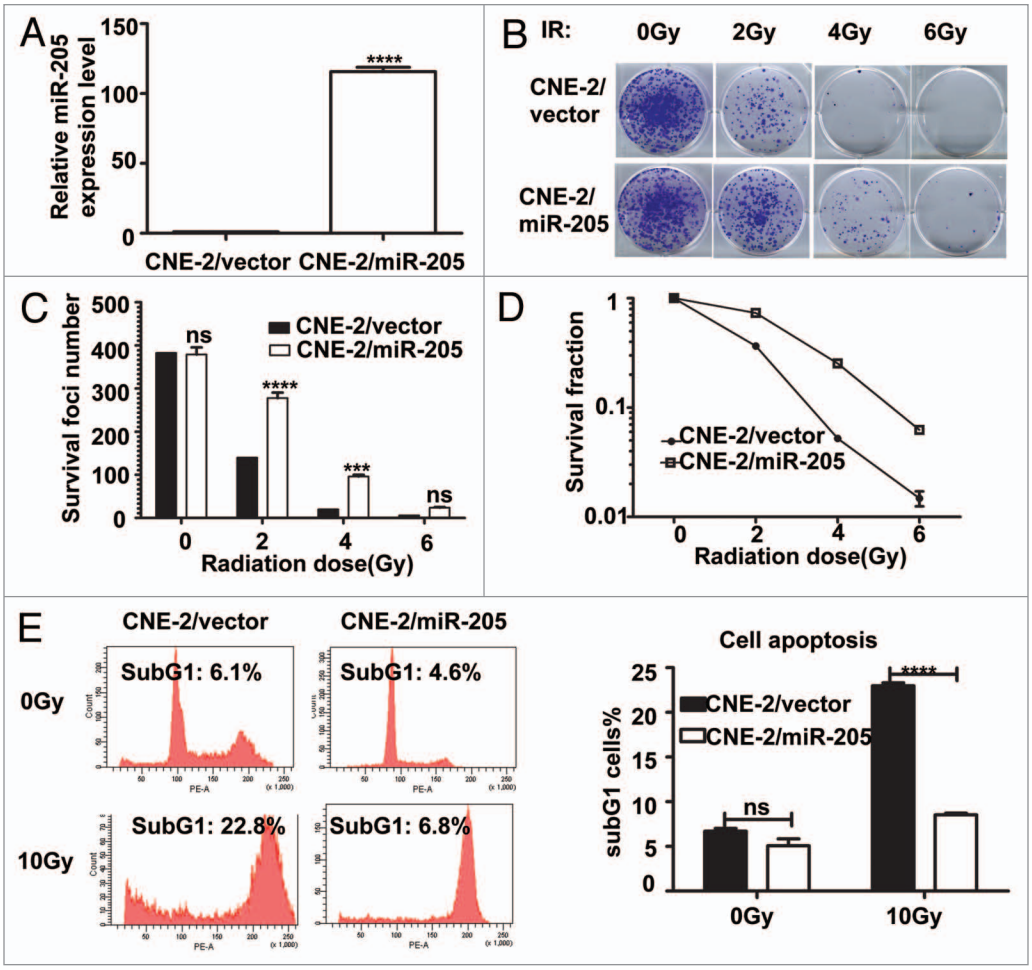

Figure 3. Expression of miR-205 in radio-sensitive cells leads to IR resistance. (A) miR-205 overexpression in CNE-2 cells. CNE-2 cells were transfected with miR-205 expressing vector. Expression of miR-205 was quantitated by q-RTPCR. Expression of miR-205 in the transduced cells was assessed by qRT-PCR with U6 RNA as an internal control. (B) CNE-2 overexpressing miR-205 becomes more IR resistant. Indicated miR-205-overexpressing CNE-2 cells were plated in triplicate and exposed to a range of IR doses (0–6 Gy). The forci-formation was indicated. (C) miR-205-overexpressing CNE-2 cells have induced numbers of forci formation. The numbers of foci-formation were presented as bar graphs. (D) miR-205-overexpressing CNE-2 cells have increased survival fraction. Survival fractions were calculated as described above based on the data from experiments in (C). (E) miR-205-overexpressing CNE-2 cells is resistant to IR-induced cell death. Indicated cells were treated with or without 10 Gy IR and the cells were stained with PI and the percentage of sub-G_1 cells was measured by flow cytometry in three independent experiments. The percentage of sub G_1 cells was presented as bar graphs.

expression of miR-205. We generated a CNE-2R cell line in which miR-205 was knocked down (CNE-2R/anti-miR-205) (**Fig.** 4). Also, control cells were generated by transducing the CNE-2R with corresponding empty lentiviral vectors. qRT-PCR confirmed that CNE-2R/anti-miR-205 cells have 50% decrease in miR-205 expression (**Fig. 4A**). We examined the effect of anti-miR-205 on the survival foci formation ability and apoptosis when exposed to IR. CNE-2R/anti-miR-205 cells had reduced foci numbers when compared with CNE-2R/vector cells (**Fig. 4B and C**). As expected, CNE-2R/anti-miR-205 cells had a worse survival rate and higher percentage of sub-G_1 when compared with CNE-2R/vector cells (**Fig. 4D and E**). Also, we used a NPC cell line CNE1, which has high levels of miR-205,[14] and is resistant to IR, for an IR-induced apoptosis experiment. We found that anti-miR-205 led to increased apoptosis after exposure to IR when compared with CNE-1/anti-vector cells (**Fig. 4F**). Together, these data confirm that knockdown of miR-205 in previously radio-resistant CNE-2R or CNE1 cells renders them radiosensitive.

MiR-205 inhibits PTEN expression by targeting PTEN 3'-UTR in NPC. Importantly, we demonstrate that 3'-UTR of human PTEN (759–765 nt) contains a miR-205 binding site. This binding site is highly conserved among different species (**Fig. 5A**). The "seed sequence" of miR-205 was perfectly complementary to the target sequence in the 3'-UTR of PTEN gene. Hybridization of miR-205 and PTEN mRNA can be predicted by RNAhybrid software (**Fig. 5B**), and the minimum free energy required for this hybridization is -28.6 kcal/mol (**Fig. 5B**).

Human PTEN gene, located in human chromosome 10q23, has been identified as one of the most frequently lost or mutated genes in several sporadic and heritable tumor types. Evidence has shown that PTEN negatively regulates cell cycle progression by dephosphorylating phosphatidylinositol-(3,4,5)-trisphosphate (PIP3) followed by inhibition of the Akt/PKB pathway that signals cells

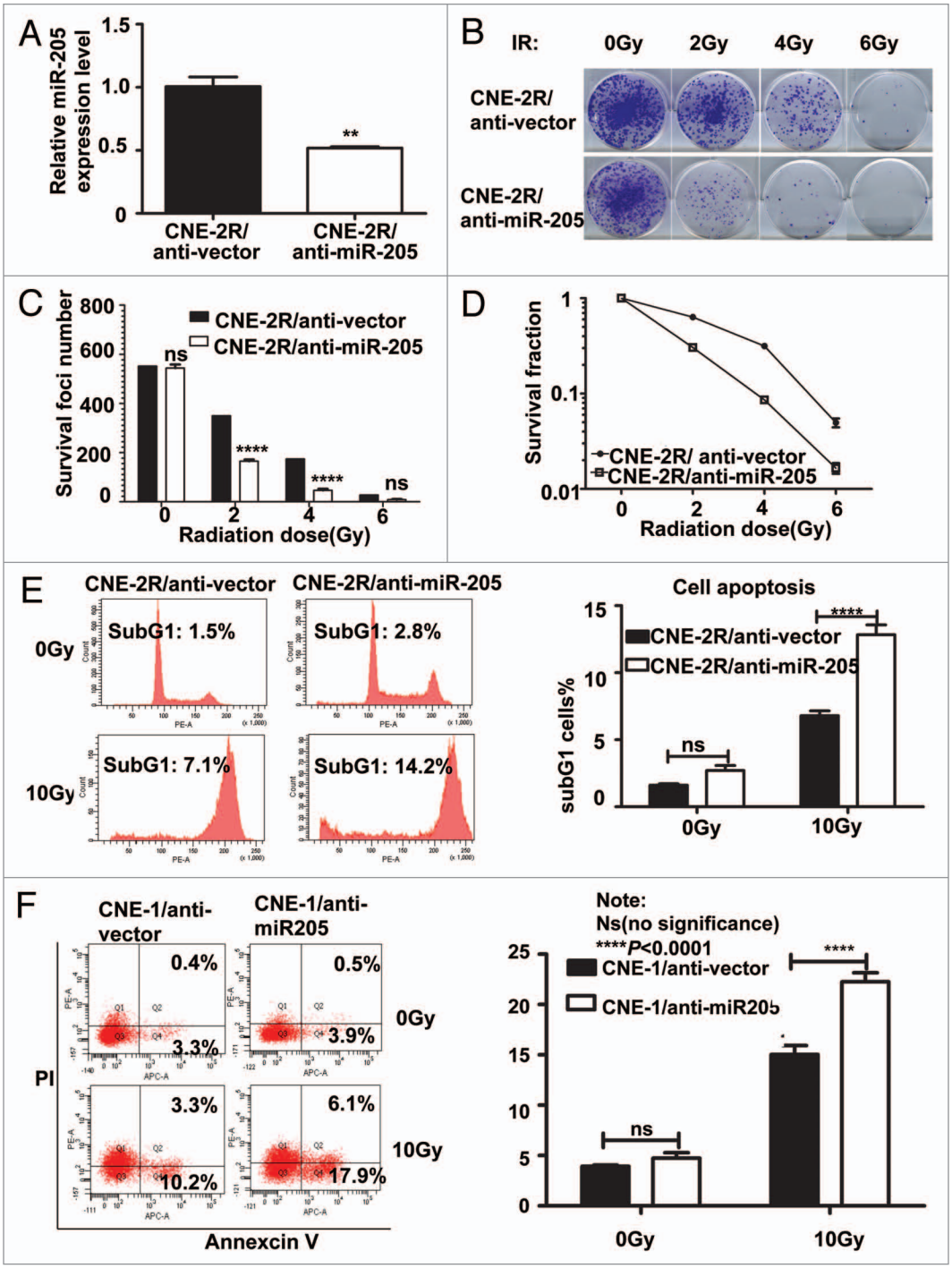

Figure 4. Suppression of Mir 205 in CNE-2R cells leads to radiosensitivity to IR-regulated cell death. (A) Lentiviral anti-miR-205 leads to miR-205 suppression in CNE-2R cells. CNE-2R cells were transfected with lenti-virus based copGFP-anti-miR-205 vector. Expression of miR-205 was quantitated by q-RTPCR. (B) CNE-2R overexpressing anti-miR-205 becomes more IR sensitive. Indicated anti-miR-205-overexpressing CNE-2R cells were plated in triplicate and exposed to a range of IR doses (0–6 Gy). The forci-formation was indicated. (C) anti-miR-205-overexpressing CNE-2R cells have reduced numbers of forci formation. The numbers of foci-formation were presented as bar graphs. (D) anti-miR-205-overexpressing CNE-2R cells have reduced survival fraction. Survival fractions were calculated as described above based on the data from experiments in (C). (E) anti-miR-205-overexpressing CNE-2R cells is sensitive to IR-induced cell death. Indicated cells were treated with or without 10 Gy IR and the cells were stained with PI for measuring the percentage of sub G_1 cells. Three independent experiments were done. The percentage of sub G_1 cells in experiment was presented as bar graphs. ns, no significance; ****$p < 0.0001$. (F) anti-miR-205-overexpressing CNE-1 cells is sensitive to IR-induced cell death. Cells were treated with or without 10 Gy IR and the cells were stained with annexin V for measuring the percentage of apoptotic cells. The percentage of apoptotic cells in experiment was presented as bar graphs. ns, no significance; ****$p < 0.0001$.

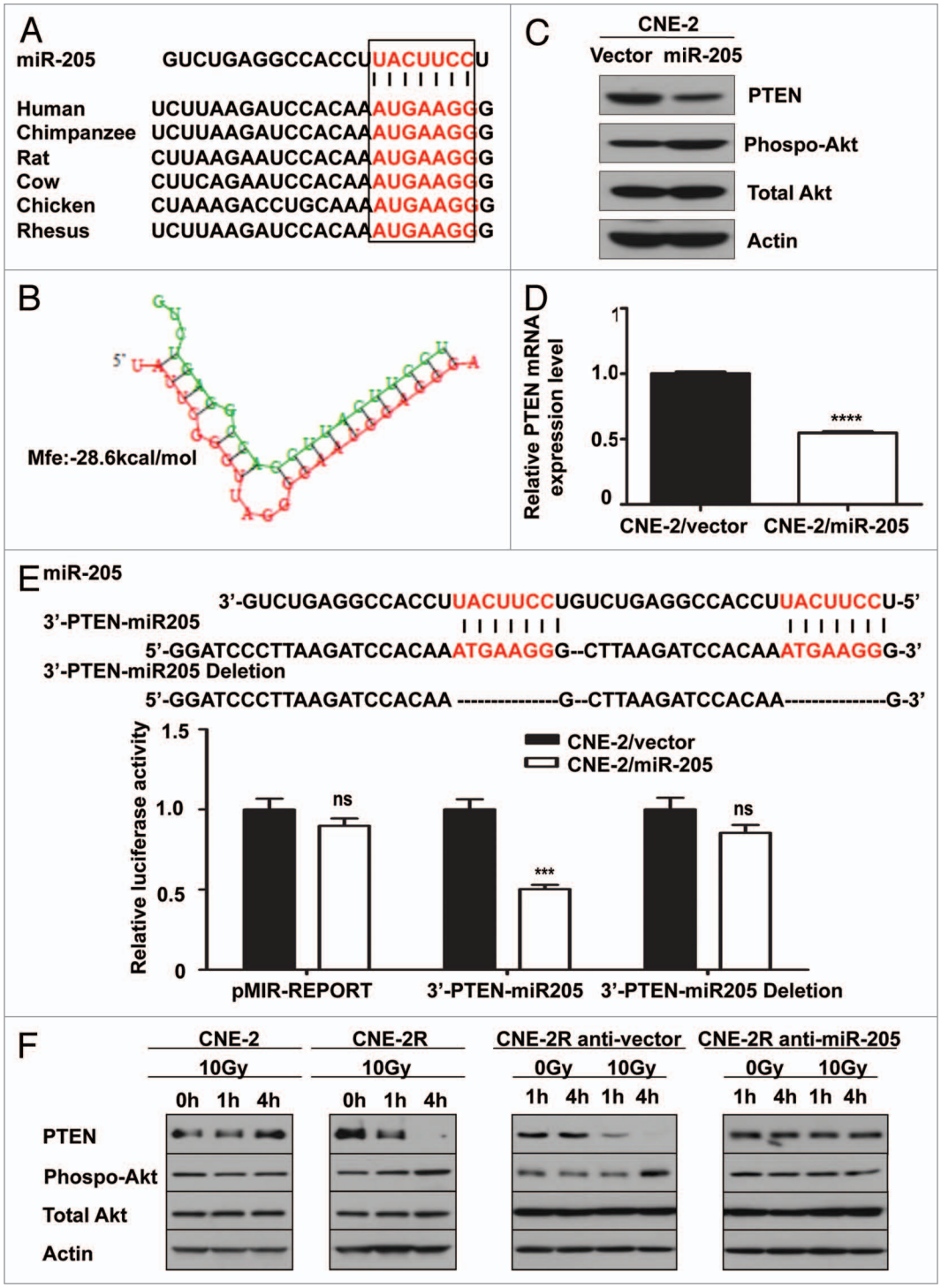

Figure 5. Suppressing the expression of miR-205 compromises the IR-induced downregulation of PTEN. (A) MiR-205 represses PTEN expression by targeting the 3'-UTR of PTEN mRNA. An miR-205 binding site within PTEN 3'UTR that is conserved in different species was predicted by TargetScan. The "seed" sequences of miR-205 complementary to PTEN are shown in red box. (B) Hybridization of miR-205 (green) and PTEN mRNA (red) was predicted by RNAhybrid software. The minimum free energy (mfe) required for this hybridization is indicated. (C) Expression of Mir 205 in CNE-2 cells leads to downregulation of PTEN and increased akt activity. Levels of PTEN protein expression and phosphorylation of Akt after transfection of miR-205 into CNE-2 cells were demonstrated by indicated antibodies. (D) PTEN mRNA levels is downregulated after miR-205 transfection. Gene expression was measured by qRT-PCR. Data were presented as mean ± SEM (n = 3). ****$p < 0.0001$. (E) Reporter gene assay. pMIR-REPORT, 3'-PTEN-miR-205 and the mutant reporter 3'-PTEN-miR-205-deletion were transfected into CNE-2/vector and CNE-2/miR-205 cells. Luciferase reporter gene activities were assayed. Data were presented as mean ± SEM of 3 experiments. ***$p < 0.001$. (F) Suppressing the expression of Mir-205 compromises the IR-induced downregulation of PTEN. Indicated cells were irradiated with 10 Gy IR or without. The lysates were immunoblotted with indicated antibodies.

for dividing and cell survival. Also, PTEN is reportedly involved in the complex response to IR via inducing cell cycle G_2/M arrest and apoptosis and in sensitizing cells to radiochemotherapy.[15,16] Accordingly, we hypothesized that PTEN is responsible for radioresistance mediated by miR-205. To address this hypothesis, we analyzed PTEN protein and mRNA level in the miR-205-overexpressing CNE-2 cell (CNE-2/miR-205), using CNE-2/vector as a control. As clearly shown by western blot analysis, the protein level of PTEN was markedly reduced in CNE-2/miR-205 compared with that in CNE-2/vector cells (**Fig. 5C**). In addition to the reduction in PTEN protein level, phosphorylation of AKT at serine 473 was increased when miR-205 was abundantly present (**Fig. 5C**). The PTEN mRNA was also significantly decreased in established CNE-2/miR-205 cells as confirmed by qRT-PCR analysis (**Fig. 5D**). These data indicate that miR-205 regulates PTEN gene expression at the transcriptional level.

Next, we examined specific targeting of PTEN by miR-205. CNE-2 cells overexpressing miR-205 and the parent control cell line CNE-2 were transfected with a luciferase reporter plasmid carrying the PTEN 3'-UTR fragment containing either the miR-205 binding site (the 3'-PTEN-miR-205) or a control plasmid. Luciferase assay results showed that expression from the PTEN reporter (3'-PTEN-miR-205) was substantially suppressed in the copGFP-miR-205 overexpressing CNE-2 cells compared with the pMIR-REPORT control plasmid transfection (**Fig. 5E**). This suppression was observed in CNE-2 cells, indicating that miR-205 inhibits PTEN expression by targeting the 3'-UTR of the PTEN gene. To verify the specificity of this inhibition, we repeated the luciferase assay by using a modified 3'-PTEN-miR-205 PTEN reporter gene in which the miR-205 seed sequence AUG AAG G was deleted to abolish binding of miR-205 with PTEN 3'-UTR. The results show that disruption of binding between miR-205 and the PTEN 3'-UTR compromises miR-205-mediated inhibition of luciferase activity (**Fig. 5E**). We conclude that miR-205 suppresses PTEN gene expression through specifically targeting 3'-UTR of this gene.

Suppressing the level of miR-205 compromises the IR-induced downregulation of PTEN. To examine the effect of IR on levels of PTEN protein expression, we exposed both CNE-2 and CNE-2R to IR for various amount of time. As shown by western blot, IR exposure resulted in repression of PTEN and activation of phosphorylation of Akt in CNE-2R (**Fig. 5F**). In contrast, the phenomenon was absent in CNE-2 cells under the same treatment (**Fig. 5F**). These data indicate that IR induces repression of PTEN, which consequently leads to phosphorylation of Akt in radio-resistant CNE-2R cells. Strikingly, inhibiting miR-205 function by miR-205 shRNA reversed suppression of PTEN protein expression in CNE-2R cells, confirming that repression of PTEN level in CNE-2R cells is under control of miR-205 (**Fig. 5F**). Because activation of phosphorylation of Akt (caused by PTEN downregulation) in CNE-2R following IR may impact on IR-induced cell survival, we then investigated whether a PI3K/Akt inhibitor sensitizes CNE-2R and miR-205 high expressing cell to IR. We found that PI3K inhibitor LY294002 treatment in CNE2R and CNE1 led to increased apoptosis after exposure to IR when compared with non-treatment controls (**Fig. 6**). Thus, LY294002 sensitizes CNE-2R and miR-205 high expressing cells, such as CNE1, to IR (**Fig. 6**). Together, our results suggest that downregulation of PTEN is involved in radioresistance of NPC and that inhibition of PI3K/Akt signaling pathway can reverse such a process.

Table 1. The difference of PTEN expression in NPC tissues with different clinical stages

	Stages I/II	Stages III/IV
Low PTEN	3	12
High PTEN	5	3

Note: Mann-Whitney U test $p < 0.046$. Clinical stages: I: T1N0M0. II: T2N0M0. III: T3N0M0; T1N1M0; T3N1M0. IV: T4N0 ~ 1M0; T1 ~ 4N2 ~ 3M0; T1 ~ 4N1 ~ 3M1.

PTEN is downregulated in late stages of NPC. It is known that NPC patients with higher clinical stages are more resistant to radiotherapy. To correlate the clinical significance of miR-205/PTEN pathway and NPC radioresistance, we performed immunohistochemistry to evaluate PTEN protein levels in paraffin-embedded tumor biopsies of NPC with definite diagnosis. Then we did a correlation analysis on the relationship between the level of tumor expression of PTEN protein and the degree of radioresistance of the tumor, which we classified by tumor stages (early clinical stages I/II vs. advanced clinical stages III/IV). The data demonstrated that PTEN was expressed in all 23 NPC tissue sections examined, and the levels of PTEN expression were correlated with the clinical stages of the patients. Specifically, the patients with lower levels of PTEN protein were found to be in more advanced clinical stages (stage III and IV) of NPC ($p = 0.046$, **Table 1**). Representative PTEN staining with different clinical stages was presented (**Fig. 7A**).

To investigate the correlation of radiotherapy with miR-205 expression in a clinical setting, we analyzed the level of miR-205 expression in patients with NPC. Fresh tumor tissues were collected before and after radiotherapy, and miR-205 expression in the tissues was determined by qRT-PCR. miR-205 expression was elevated in all the patients after radiotherapy (**Fig. 7B**), recapitulating the biochemical studies. These data strongly suggest that the miR-205/PTEN pathway has an important role in radioresistance in a clinical setting.

Discussion

Intrinsic and acquired resistance to radiotherapy is a major clinical obstacle in treating cancers. Although mechanisms for cellular radioresistance have been extensively investigated on established radio-resistant cell models, including, but not limited to, MGR2R,[17] WiDr,[18] RRC[19] and H69SCLCR,[20] they are still not fully understood. Recently, accumulating data have shown aberrant expression of certain miRNAs in every tumor examined. The importance of miRNAs as potential prognostic indicators for cancer is underscored by their functions in regulating fundamental cellular processes, such as cell proliferation, differentiation and apoptosis.[21] Yet, the role of miRNAs in radioresistance of NPC is still obscure. In this study, through establishment of a radio-resistant cell model, CNE-2R, we find that

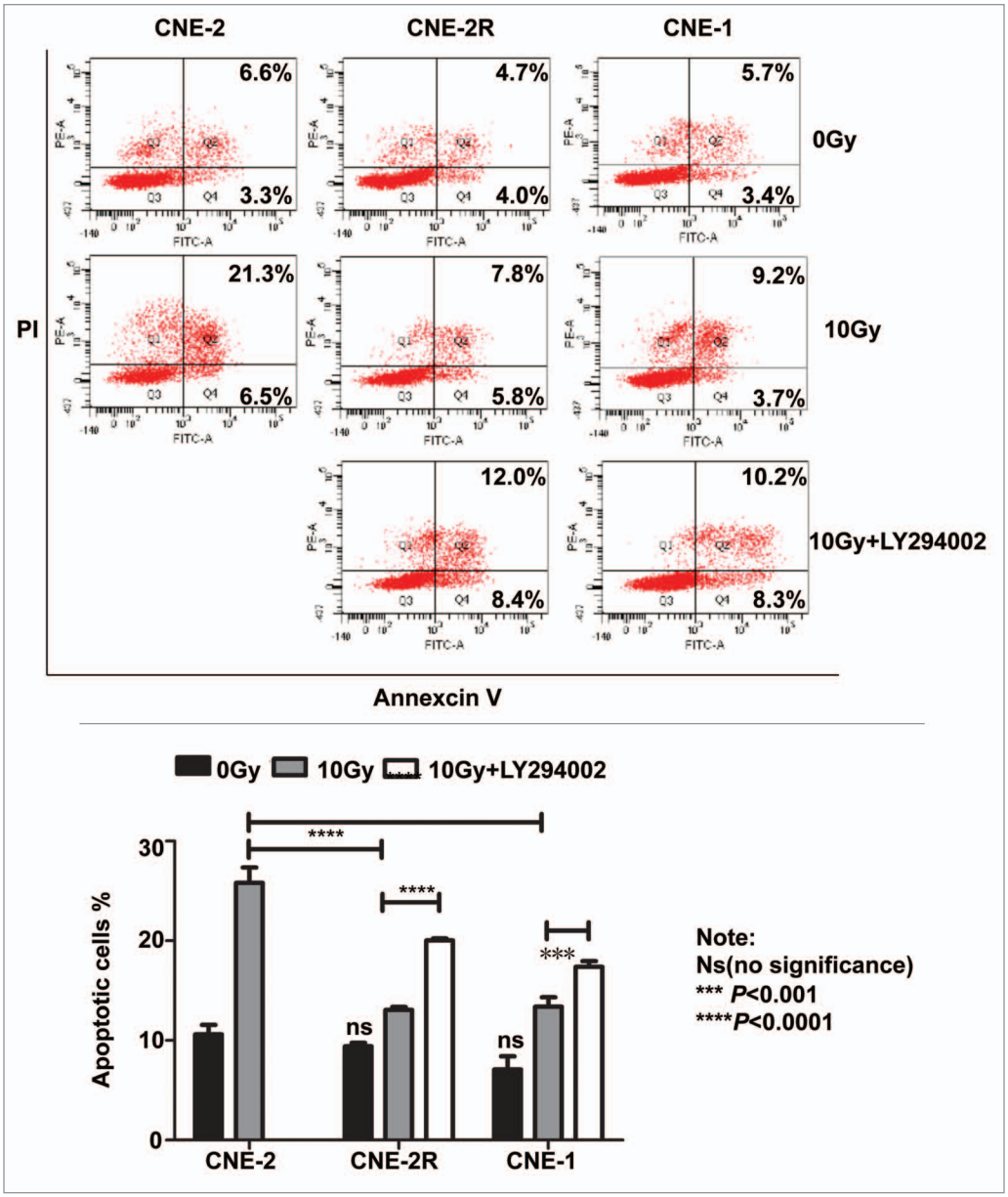

Figure 6. Inhibition of PI3K/Akt signaling pathway can reverse radioresistance of NPC. Indicated cells were treated with or without 10 μM Ly294002 in the presence of IR. The cells were stained with annexin V for measuring the percentage of apoptotic cells. The percentage of apoptotic cells in experiment was presented as bar graphs. ns, no significance; ****p < 0.0001.

IR induces miR-205 expression, and this induction consequently inhibits expression of the tumor suppressor PTEN by directly targeting the 3'-UTR of PTEN gene in NPC. We also find that miR-205-mediated inhibition of PTEN expression subsequently activates the PI3K/Akt pathway, leading to tumor cell proliferation and inhibition of tumor cell apoptosis after IR, resulting in NPC radioresistance. Our data indicate a strong link between IR-inducible miR-205, PTEN expression and radioresistance in NPC (**Fig. 6C**). More importantly, we find that the miR-205/PTEN pathway in tumor tissues is closely correlated with radiotherapy/clinical stage of the patients with NPC, suggesting that miR-205/PTEN pathway might be a valuable prognosis indicator and a novel target for NPC therapy.

Tumor cell populations in tissue usually have a variety of radiosensitivity, and previous studies have shown successful selection of radio-resistant variants by exposing the cells to an appropriate regime of irradiation.[22] We chose the radiosensitive NPC cell line CNE-2 as a parent cell line to better mimic the clinical situation, as the majority of NPCs are pathohistologically undifferentiated non-keratinizing carcinomas that are sensitive to radiation.[23] Working with such a radiosensitive cell line, we use increasing doses or IR for successful selection of stably radio-resistant cells, CNE-2R. The radioresistance of CNE-2R indicates that CNE-2R cells mount an adaptive response to IR. The stable maintenance of radioresistance in CNE-2R for over 50 passages without IR suggests that the adaptation results in a

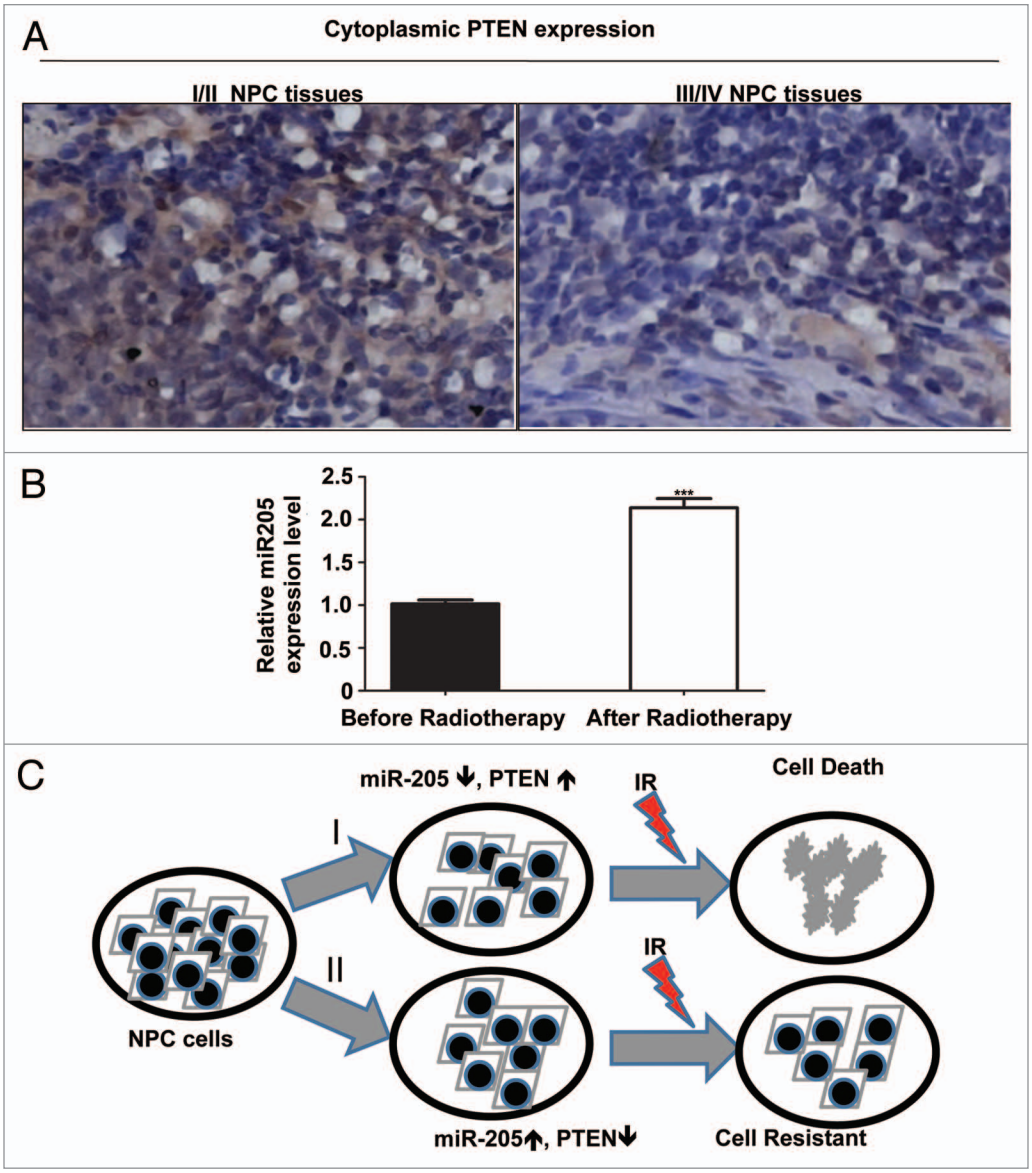

Figure 7. PTEN is downregulated in late stages of NPC. (A) High PTEN expression correlates with late stages in NPC. NPC cancer tissues were immunostained with anti-PTEN. Micrographs of two representative NPC cancer specimens were shown (original magnification, 200x). (B) Upregulaion of miR-205 is observed in NPC tissue after radiotherapy. qRT-PCR was used to quantify miR-205 expression levels in the NPC tissues obtained before and after radiotherapy. Data were presented as mean ± SEM of 3 experiments. ***$p < 0.001$, compared with before radiotherapy.

complete phenotype change of the tumor cells. Our study also demonstrates that increasing doses of IR is an advantageous strategy that does not sterilize the cells, but allows simultaneous growth of more radio-resistant cells and favors emergence of a stable radio-resistant cell line under selective pressure.

In our study, we demonstrate that CNE-2R and CNE-2 cells have differential miR expression profiles. miR 205 is particularly elevated in the CNE-2R cell line. Interestingly, miR-205 can regulate PTEN gene degradation. The miR-205-PTEN axis in radiosensitivity is very specific, as miR-205 expression not only suppresses PTEN mRNA and protein level in CNE-2 cells but also causes CNE-2 cells to become resistant to IR. On the other hand, blocking endogenous miR-205 in CNE-2R cells abrogates the suppression of PTEN expression and confers radiosensitivity to the cells. PTEN is a phosphatase that can affect the activity of Akt, a regulator involved in cell survival. Although IR can induce PI3K-Akt activation in many radio-resistant cell types, and activation of the PI3K-Akt signaling pathway has been correlated with radioresistance,[24] the signaling pathway has not been fully elucidated. In this study, IR induction of miR-205 not only suppresses PTEN protein level but also results in activation of the Akt signaling pathway in NPC when exposed to IR. Our finding provides insights into the mechanism for explaining IR-inducible Akt activation and subsequent cell survival. Importantly, we were able to demonstrate that PI3K/Akt inhibitor,[25,26] which is also effective in regulating effectiveness in chemotherapeutic drugs, can reverse the radioresistance of NPC.

Here, our studies show that miR-205 acts as an important gene responding early to IR and can increase radioresistance in NPC by directly targeting PTEN. Paradoxically, miR-205 was reported to act as a tumor suppressor that inhibits cell growth, invasion and migration of cancers.[27-31] It was also found to inhibit EMT, an essential early step in tumor metastasis that can contribute to radioresistance and chemoresistance by directly targeting ZEB1 and SIP1.[32,33] This discrepancy about the role of miR-205 in cancer could reflect the complexity of regulation function of miRNAs, a fine-tuner of gene expression in cells. It is possible that miR-205 performs context-specific functions depending on the microenvironment of the cells and the type of the tumor.

Studies from several groups have concluded that IR can upregulate many genes but suppress more genes. The suppressed genes include those involved in proliferation and oxidative stress. Our data shed light on regulation of miRNA expression, which alters cellular gene expression in NPC cells. It is important to point out that several miRNAs are also differentially expressed in CNE2R cells. Some of these miRNAs remained to be further investigated and could add more understanding about the underlying mechanism for resistance of NPC to stress of IR.

PTEN is a key regulator of cell apoptosis. Cells losing PTEN are partially resistant to numerous apoptotic stimuli.[34] We found that the level of PTEN expression was reduced in tumor tissues with advanced clinical stages of NPC (**Fig. 6**). NPC patients with higher clinical stages are more resistant to radiotherapy and have worse prognosis because of local lymphoid node and distant metastasis. On the basis of our studies, we propose that loss of PTEN expression is associated with radioresistance of NPC. Consistent with the results of our cell line studies on the miR-205/PTEN pathway, we demonstrate elevated miR-205 expression in the tumor tissues from NPC patients after radiotherapy, which suggests that miR-205/PTEN pathway plays a critical role in radioresistance of NPC patients. Additional prospective, controlled studies could evaluate the value of miR-205/PTEN as a molecular marker in NPC for predicting radiosensitivity and prognosis.

Materials and Methods

Cell culture and reagents. Human undifferentiated non-keratinizing nasopharyngeal carcinoma cell line CNE-2 was obtained from Experiment Animal Center of Sun Yat-Sen University. Both CNE-2R and CNE-2 cells were cultured in RPMI-1640 medium (Invitrogen) supplemented with 10% fetal bovine serum, penicillin G 100 units/ml, streptomycin 100 ug/ml and amphotericin B 0.25 ug/ml in a humidified atmosphere of 5% CO_2 at 37°C. DMSO, crystal violet and propidium iodide (PI) were purchased from Sigma Chemical Co. PowerPlex® 16 kit was purchased from Promega Co., and the μParaflo™ microfluidic chip was purchased from LC Sciences Biochemical and Chemical Product Co. MiRNA primers and TaqMan® MicroRNA Reverse Transcription Kits, the pre-miR-control, precursor miR-205, anti-miR negative control and anti-miR-205 inhibitor were products from Applied Biosystems Co.

Cell growth analysis. Cells were plated in 24-well culture plates (2.5 x 10^4/well). After incubation for 24 h, the cells were irradiated with 2 Gy. Cell growth was monitored by counting cell numbers at various time intervals. Three independent experiments were done in triplicate.

Survival foci formation assay. Cells in exponential growth phase were plated into a six-well plate at 3,000 cells/well and then incubated for 24 h to allow settling. The cells were treated with a range of IR doses (0, 2, 4 Gy and 6 Gy, Nasatron (Cs-137) irradiator). When most cell clones had reached > 50 cells, they were stained with 0.06% crystal violet.

Flow cytometry. To determine IR-induced cell death, cells were treated with or without 10 Gy IR. At 48 h post-irradiation, the cells were harvested, fixed and stained with RNase and 50 μg/mL of PI for 30 min. Fluorescence signal from PI was measured at 630 nm, with 10,000 events acquired per sample. Data were collected using BD FACSCANTO II flow cytometer (BD Biosciences). For Annexin V staining, cells were resuspended in 1x binding buffer (Axxora Platform) and incubated with FITC-conjugated annexin V for 15 min. at room temperature in the dark using the FITC-annexin V apoptosis detection kit. Cells were immediately analyzed on fluorescence activated cell sorting (FACS) calibur flow cytometer (Becton Dickinson Immunocytometry System) using the CellQuest Pro Software and WINMDI 2.9 software.

Microarray for miRNAs. MiRNA microarray analysis was performed on CNE-2R and CNE-2 cells. Briefly, 2 to 5 mg total RNA were isolated, size fractioned and labeled with Cy3 or Cy5. Paired labeled samples were hybridized to a dual-channel microarray using the μParaflo™ microfluidic chips based on Sanger miRBase release 10.1. Raw data were normalized by the LOWESS method on the background-subtracted data.

qRT-PCR. qRT-PCR was performed to detect miRNAs expression using TaqMan® miRNA reverse transcription kit and TaqMan miRNA assay kits (Applied Biosystems), following the manufacturer's protocol. Expression levels for each gene were normalized to that of rRNA U6 and then converted into relative values calculated by the comparative CT method. qRT-PCR was also used to measure mRNA expression with TaqMan® miRNA reverse transcription kit and sybergreen supermix (Biorad). PTEN mRNA expression were examined using specific primers (forward: 5'-TGG ATT CGA CTT AGA CTT GAC CT; reverse: 5'-TTT GGC GGT GTC ATA ATG TCT T). Actin mRNA was used as an internal control to normalize PTEN mRNA level.

Western blotting. Western blotting was performed as previously described in reference 35, with primary antibodies against PTEN (SantaCruz), phospho-Akt (Cell Signaling), total Akt (Cell Signaling), tubulin (Sigma) or actin (Santa Cruz) and an HRP-conjugated secondary antibody (Thermo Scientific), followed by enhanced chemiluminescence detection.

Generation of stable cell lines. Human pre-miRNA expression constructs Lenti-miR-205 MI0000285, anti-miR-205 miRNA construct MZIP205-PA-1, precursor control lentivector (CD511B-1) and anti-miR scramble control lentiviral vector (SI505A-1) were purchased from System Biosciences. To generate stable miR-205 overexpressing and miR-205 knockdown

cell lines, CNE-2R and CNE-2 were infected with lentiviral transduction particles containing copGFP-miR-205 plasmid, copGFP-precursor vector, copGFP-anti-miR-205 plasmid (miR-205shRNA) or anti-miR scramble control lentiviral vector. Cells were grown in the presence of 4 μg/mL puromycin for selection of stably transfected clones. Single clones were picked to generate monoclonal cell lines.

Plasmid constructions. The miRNA reporter constructs, (3'-PTEN-miR205 and 3'-PTEN-miR205 deletion) were obtained by directly inserting the annealed oligonucleotides into the pMIR-REPORT luciferase miRNA expression reporter vector (Ambion) between the SacI and HindIII sites. The sense and antisense strands of the oligonucleotides (3'-PTEN-miR205 forward: 5'-C-CCC TTC ATT TGT GGA TCT TAA GCC CTT CAT TTG TGG ATC TTA AGG GAT CC-A-3'; 3'-PTEN-miR205 reverse: 5'-AGC TTG GAT CCC TTA AGA TCC ACA AAT GAA GGG TTA AGA TCC ACA AAT GAA GGG GAG CT-3'; 3'-PTEN-miR205 deletion forward: 5'-C-CTG TGG ATC TTA AGC TGT GGA TCT TAA GGG ATC C-A-3'; 3'-PTEN-miR205 deletion reverse: 5'-AGC TTG GAT CCC TTA AGA TCC ACA GCT TAA GAT CCA CAG GAG CT-3') were used for annealing and cloning.

Luciferase assays. The two luciferase reporters, 3'-PTEN-miR205 and 3'-PTEN-miR205 deletion, were transfected into CNE-2/vector and CNE-2/miR205, respectively using Lipofectamine 2000 (Invitrogen). pMIR-REPORT™ β-galactosidase reporter control vector (Ambion) was cotransfected for normalization of transfection efficiency. Luciferase and β-galactosidase activities were measured as described previously in reference 36.

Immunohistochemistry. PTEN expression was detected immunohistochemically on 23 paraffin-embedded NPC tissue sections from patients at Sun Yat-Sen University Cancer Center. In brief, deparaffinized sections were treated at 100°C in a steamer containing 10 mM citrate buffer (pH 6.0) for 60 min and then immersed in 3% hydrogen peroxide solution for 10 min to inhibit endogenous peroxidase activity, followed byincubation of the sections in 5% BSA to block nonspecific binding. Then the sections were incubated with primary antibodies against PTEN (1:1,125 dilution, Cell Signaling, #9188) at 4°C overnight. Standard avidin-biotin immunohistochemical analysis of the sections was done following the manufacturer's instruction (Boster, #SA1022). And diaminobenzidne was used as a chromogen and hematoxylin for counterstaining. The PTEN staining in nucleus and the cytoplasm of the tumor cells was scored separately and added up for each case as described previously in reference 1. A minimum five high-power fields were chosen randomly and > 1,000 cells were counted for each section.

Statistics. The Student's t-test was used to evaluate the significant difference of two groups of data in all the pertinent experiments. A p-value < 0.05 (using a two-tailed paired t-test) was thought to be significantly different for two groups of data. For immunohistochemical data, Mann-Whitney U test was performed with the statistical package SPSS 13.0. to evaluate the difference of PTEN expression levels in NPC tissues of early clinical stages (I/II) and advanced clinical stages (III/IV). A two-sided $p < 0.05$ was considered significant.

Disclosure of Potential Conflicts of Interest

No potential conflicts of interest were disclosed.

Acknowledgements

This work was supported in part by the NIHRO1CA (089266), Cancer Center Core Grant (CA16672), National Natural Science Foundation of China (NO: 30670627; 30870745; 81071837), National Natural Science Foundation of Guangdong Province, China (NO: 9251008901000005; 06021210), the International Program Fund of 985 Project, Sun Yat-Sen University, China and Exchange Visitor Program (NO: P-1-10254), the University of Texas MD Anderson Cancer Center.

References

1. Feng XP, Yi H, Li MY, Li XH, Yi B, Zhang PF, et al. Identification of biomarkers for predicting nasopharyngeal carcinoma response to radiotherapy by proteomics. Cancer Res 2010; 70:3450-62; PMID:20406978; http://dx.doi.org/10.1158/0008-5472.CAN-09-4099.
2. DeNittis AS, Liu L, Rosenthal DI, Machtay M. Nasopharyngeal carcinoma treated with external radiotherapy, brachytherapy and concurrent/adjuvant chemotherapy. Am J Clin Oncol 2002; 25:93-5; PMID:11823706; http://dx.doi.org/10.1097/00000421-200202000-00020.
3. Chang JT, Ko JY, Hong RL. Recent advances in the treatment of nasopharyngeal carcinoma. J Formos Med Assoc 2004; 103:496-510; PMID:15318271.
4. Mostafa E, Nasar MN, Rabie NA, Ibrahim SA, Barakat HM, Rabie AN. Induction chemotherapy with paclitaxel and cisplatin, followed by concomitant cisplatin and radiotherapy for the treatment of locally advanced nasopharyngeal carcinoma. J Egypt Natl Canc Inst 2006; 18:348-56; PMID:18301458.
5. Gupta AK, McKenna WG, Weber CN, Feldman MD, Goldsmith JD, Mick R, et al. Local recurrence in head and neck cancer: relationship to radiation resistance and signal transduction. Clin Cancer Res 2002; 8:885-92; PMID:11895923.
6. Qin X, Wang X, Wang Y, Tang Z, Cui Q, Xi J, et al. MicroRNA-19a mediates the suppressive effect of laminar flow on cyclin D1 expression in human umbilical vein endothelial cells. Proc Natl Acad Sci USA 2010; 107:3240-4; PMID:20133739; http://dx.doi.org/10.1073/pnas.0914882107.
7. Radojicic J, Zaravinos A, Vrekoussis T, Kafousi M, Spandidos DA, Stathopoulos EN. MicroRNA expression analysis in triple-negative (ER, PR and Her2/neu) breast cancer. Cell Cycle 2011; 10:507-17; PMID:21270527; http://dx.doi.org/10.4161/cc.10.3.14754.
8. Zhang L, Deng T, Li X, Liu H, Zhou H, Ma J, et al. microRNA-141 is involved in a nasopharyngeal carcinoma-related genes network. Carcinogenesis 2010; 31:559-66; PMID:20053927; http://dx.doi.org/10.1093/carcin/bgp335.
9. Alajez NM, Lenarduzzi M, Ito E, Hui AB, Shi W, Bruce J, et al. MiR-218 suppresses nasopharyngeal cancer progression through downregulation of survivin and the SLIT2-ROBO1 pathway. Cancer Res 2011; 71:2381-91; PMID:21385904; http://dx.doi.org/10.1158/0008-5472.CAN-10-2754.
10. Lu J, He ML, Wang L, Chen Y, Liu X, Dong Q, et al. MiR-26a inhibits cell growth and tumorigenesis of nasopharyngeal carcinoma through repression of EZH2. Cancer Res 2011; 71:225-33; PMID:21199804; http://dx.doi.org/10.1158/0008-5472.CAN-10-1850.
11. Sengupta S, den Boon JA, Chen IH, Newton MA, Stanhope SA, Cheng YJ, et al. MicroRNA 29c is downregulated in nasopharyngeal carcinomas, upregulating mRNAs encoding extracellular matrix proteins. Proc Natl Acad Sci USA 2008; 105:5874-8; PMID:18390668; http://dx.doi.org/10.1073/pnas.0801130105.
12. Takamizawa J, Konishi H, Yanagisawa K, Tomida S, Osada H, Endoh H, et al. Reduced expression of the let-7 microRNAs in human lung cancers in association with shortened postoperative survival. Cancer Res 2004; 64:3753-6; PMID:15172979; http://dx.doi.org/10.1158/0008-5472.CAN-04-0637.
13. Weidhaas JB, Babar I, Nallur SM, Trang P, Roush S, Boehm M, et al. MicroRNAs as potential agents to alter resistance to cytotoxic anticancer therapy. Cancer Res 2007; 67:11111-6; PMID:18056433; http://dx.doi.org/10.1158/0008-5472.CAN-07-2858.
14. Wang X, Yang H, Guo Y, Liang Z, Zhao R, Xia Y, et al. Discrepancy of microRNA in different radio-resistant nasopharyngeal carcinoma cells. Chinese Journal of Pathophysiology 2007; 23:1045-8.
15. Lee JJ, Kim BC, Park MJ, Lee YS, Kim YN, Lee BL, et al. PTEN status switches cell fate between premature senescence and apoptosis in glioma exposed to ionizing radiation. Cell Death Differ 2011; 18:666-77; PMID:21072054; http://dx.doi.org/10.1038/cdd.2010.139.

16. Park JK, Jung HY, Park SH, Kang SY, Yi MR, Um HD, et al. Combination of PTEN and gamma-ionizing radiation enhances cell death and G(2)/M arrest through regulation of AKT activity and p21 induction in non-small-cell lung cancer cells. Int J Radiat Oncol Biol Phys 2008; 70:1552-60; PMID:18374229; http://dx.doi.org/10.1016/j.ijrobp.2007.11.069.
17. Cheng JJ, Hu Z, Xia YF, Chen ZP. Radio-resistant subline of human glioma cell line MGR2R induced by repeated high dose X-ray irradiation. Ai Zheng 2006; 25:45-50; PMID:16405748.
18. Virsik-Köpp P, Hofman-Hüther H, Rave-Fränk M, Schmidberger H. The effect of wortmannin on radiation-induced chromosome aberration formation in the radio-resistant tumor cell line WiDr. Radiat Res 2005; 164:148-56; PMID:16138421; http://dx.doi.org/10.1667/RR3396.1.
19. Lee HC, Kim DW, Jung KY, Park IC, Park MJ, Kim MS, et al. Increased expression of antioxidant enzymes in radio-resistant variant from U251 human glioblastoma cell line. Int J Mol Med 2004; 13:883-7; PMID:15138630.
20. Henness S, Davey MW, Harvie RM, Davey RA. Fractionated irradiation of H69 small-cell lung cancer cells causes stable radiation and drug resistance with increased MRP1, MRP2 and topoisomerase IIalpha expression. Int J Radiat Oncol Biol Phys 2002; 54:895-902; PMID:12377343; http://dx.doi.org/10.1016/S0360-3016(02)03037-7.
21. Slack FJ, Weidhaas JB. MicroRNA in cancer prognosis. N Engl J Med 2008; 359:2720-2; PMID:19092157; http://dx.doi.org/10.1056/NEJMe0808667.
22. Russell J, Wheldon TE, Stanton P. A radio-resistant variant derived from a human neuroblastoma cell line is less prone to radiation-induced apoptosis. Cancer Res 1995; 55:4915-21; PMID:7585530.
23. Guo C, Pan ZG, Li DJ, Yun JP, Zheng MZ, Hu ZY, et al. The expression of p63 is associated with the differential stage in nasopharyngeal carcinoma and EBV infection. J Transl Med 2006; 4:23; PMID:16729897; http://dx.doi.org/10.1186/1479-5876-4-23.
24. Li HF, Kim JS, Waldman T. Radiation-induced Akt activation modulates radioresistance in human glioblastoma cells. Radiat Oncol 2009; 4:43; PMID:19828040; http://dx.doi.org/10.1186/1748-717X-4-43.
25. Steelman LS, Navolanic P, Chappell WH, Abrams SL, Wong EW, Martelli AM, et al. Involvement of Akt and mTOR in chemotherapeutic- and hormonal-based drug resistance and response to radiation in breast cancer cells. Cell Cycle 2011; 10:3003-15; PMID:21869603; http://dx.doi.org/10.4161/cc.10.17.17119.
26. Chappell WH, Steelman LS, Long JM, Kempf RC, Abrams SL, Franklin RA, et al. Ras/Raf/MEK/ERK and PI3K/PTEN/Akt/mTOR inhibitors: rationale and importance to inhibiting these pathways in human health. Oncotarget 2011; 2:135-64; PMID:21411864.
27. Wu H, Zhu S, Mo YY. Suppression of cell growth and invasion by miR-205 in breast cancer. Cell Res 2009; 19:439-48; PMID:19238171; http://dx.doi.org/10.1038/cr.2009.18.
28. Gregory PA, Bert AG, Paterson EL, Barry SC, Tsykin A, Farshid G, et al. The miR-200 family and miR-205 regulate epithelial to mesenchymal transition by targeting ZEB1 and SIP1. Nat Cell Biol 2008; 10:593-601; PMID:18376396; http://dx.doi.org/10.1038/ncb1722.
29. Gandellini P, Folini M, Longoni N, Pennati M, Binda M, Colecchia M, et al. miR-205 Exerts tumor-suppressive functions in human prostate through down-regulation of protein kinase Cepsilon. Cancer Res 2009; 69:2287-95; PMID:19244118; http://dx.doi.org/10.1158/0008-5472.CAN-08-2894.
30. Song H, Bu G. MicroRNA-205 inhibits tumor cell migration through downregulating the expression of the LDL receptor-related protein 1. Biochem Biophys Res Commun 2009; 388:400-5; PMID:19665999; http://dx.doi.org/10.1016/j.bbrc.2009.08.020.
31. Iorio MV, Visone R, Di Leva G, Donati V, Petrocca F, Casalini P, et al. MicroRNA signatures in human ovarian cancer. Cancer Res 2007; 67:8699-707; PMID:17875710; http://dx.doi.org/10.1158/0008-5472.CAN-07-1936.
32. Gregory PA, Bracken CP, Bert AG, Goodall GJ. MicroRNAs as regulators of epithelial-mesenchymal transition. Cell Cycle 2008; 7:3112-8; PMID:18927505; http://dx.doi.org/10.4161/cc.7.20.6851.
33. Kurrey NK, Jalgaonkar SP, Joglekar AV, Ghanate AD, Chaskar PD, Doiphode RY, et al. Snail and slug mediate radioresistance and chemoresistance by antagonizing p53-mediated apoptosis and acquiring a stem-like phenotype in ovarian cancer cells. Stem Cells 2009; 27:2059-68; PMID:19544473; http://dx.doi.org/10.1002/stem.154.
34. Stambolic V, MacPherson D, Sas D, Lin Y, Snow B, Jang Y, et al. Regulation of PTEN transcription by p53. Mol Cell 2001; 8:317-25; PMID:11545734; http://dx.doi.org/10.1016/S1097-2765(01)00323-9.
35. Su CH, Zhao R, Zhang F, Qu C, Chen B, Feng YH, et al. 14-3-3sigma exerts tumor-suppressor activity mediated by regulation of COP1 stability. Cancer Res 2011; 71:884-94; PMID:21135113; http://dx.doi.org/10.1158/0008-5472.CAN-10-2518.
36. Qin L, Zhang X, Zhang L, Feng Y, Weng GX, Li MZ, et al. Downregulation of BMI-1 enhances 5-fluorouracil-induced apoptosis in nasopharyngeal carcinoma cells. Biochem Biophys Res Commun 2008; 371:531-5; PMID:18452707; http://dx.doi.org/10.1016/j.bbrc.2008.04.117.